JOURNAL OF ADVANCED TRANSPORTATION
J. Adv. Transp. 2016; **50**:1090–1110
Published online 12 June 2016 in Wiley Online Library (wileyonlinelibrary.com). DOI: 10.1002/atr.1391

A network enhancement model with integrated lane reorganization and traffic control strategies

Jing Zhao[1], Yue Liu[2]* and Peng Li[2]

[1]*University of Shanghai for Science and Technology, Shanghai, PR China*
[2]*Department of Civil and Environmental Engineering, University of Wisconsin at Milwaukee, Milwaukee, WI, USA*

SUMMARY

Lane reorganization strategies such as lane reversal, one-way street, turning restriction, and cross elimination have demonstrated their effectiveness in enhancing transportation network capacity. However, how to select the most appropriate combination of those strategies in a network remains challenging to transportation professionals considering the complex interactions among those strategies and their impacts on conventional traffic control components. This article contributes to developing a mathematical model for a traffic equilibrium network, in which optimization of lane reorganization and traffic control strategies are integrated in a unified framework. The model features a bi-level structure with the upper-level model describing the decision of the transportation authorities for maximizing the network capacity. A variational inequality (VI) formulation of the user equilibrium (UE) behavior in choosing routes in response to various strategies is developed in the lower level. A genetic algorithm (GA) based heuristic is used to yield meta-optimal solutions to the model. Results from extensive numerical analyses reveal the promising property of the proposed model in enhancing network capacity and reducing congestion. Copyright © 2016 John Wiley & Sons, Ltd.

KEY WORDS: lane reorganization; network optimization; capacity enhancement; traffic management; bi-level programming

1. INTRODUCTION

How to efficiently utilize the existing transportation network has been one of the most important issues faced by transportation professionals as congestion on roadways in many cities across the world continues getting worse because of increasing traffic volumes. Reorganization of current roadway lane configurations through traffic management strategies can significantly reduce the construction cost of building new roads and has proved to be effective to increase the capacity of transportation network. In review of literature, commonly adopted lane reorganization strategies for network enhancement include turning restriction, lane reversal, cross elimination, and one-way street operation [1].

Turning restriction is one of the most commonly used strategies to improve the capacity of signalized intersections in an urban network [2]. The resulting capacity increase is because of the reduced number of signal phases and less lost time. However, vehicles in prohibited movements are forced to detour, which may induce extra driving distances in the network. In the NCHRP Report 457 [3], the guidelines to identify the conditions for left-turn restriction at existing intersections have been proposed; however where to implement turning restrictions was not discussed in the report. Some researchers in recent years have formulated discrete network design problems with a bi-level structure to optimize turning restriction settings in the transportation network [4, 5]. Other studies [6] attempt to eliminate conflicts between movements at an intersection and convert signalized intersections into uninterrupted flow ones (also called crossing

*Correspondence to: Yue Liu, Department of Civil and Environmental Engineering, University of Wisconsin at Milwaukee, P.O. Box 784, Milwaukee, WI, USA. E-mail: liu28@uwm.edu

elimination). Liu and Luo [7] optimized the distribution of signal control and uninterrupted flow intersections with resource constraints in static and dynamic network settings. Integrated models [8, 9] were also proposed to combine crossing elimination and lane reversal strategies during emergency evacuation.

Lane reversal (also called tidal flow) has long been used across the world to accommodate frequent and predictable unbalanced traffic demand during peak periods [10], special event management [11], and emergency evacuation [12, 13]. The key idea is to configure the lanes of a roadway to match available capacity with traffic demand. A handful of bi-level network models have been formulated to optimize the setting and selection of lane reversals while accounting for various types of route choice behaviors of network users [14–16]. Karoonsoontawong and Lin [17] further developed time-varying reversibility with different reversibility durations for various candidate link pairs in a bi-level program model, such that the optimal starting times and the optimal reversibility durations for candidate link pairs can be determined for peak-period traffic management on a daily basis.

An extreme case of the lane reversal is the one-way street strategy in which the conversion takes place in the entire roadway. Experimental studies have quantified the trip-serving capacity of the one-way street strategy [18–20]; however those results tend to be site-specific and generalization to other networks cannot be made. Gayah and Daganzo [21] compared the trip-serving capacities of one-way and two-way networks based on macroscopic analyses. It was found that two-way networks can serve more trips per unit time than one-way networks when average trip lengths are short. Similar to the turning restriction strategy, one-way street is not always beneficial because of the resulting extra vehicle detour distance. Realizing this, some researchers have developed optimization models to select the most appropriate segments for one-way traffic organization [22–24].

As above stated, lane reorganization strategies have been used for several decades and much is known about their effectiveness, feasibility, and safety. However, few efforts have been made to investigate the interactions among those strategies as well as their combinational impacts on the transportation network. Furthermore, implementation of lane reorganization strategies may also affect other conventional traffic management and control components in the network, such as lane channelization and signal timings at intersections. Neglect of such interactions may result in non-optimal design results and unsatisfactory operational performances in the network.

To remedy this deficiency, it is necessary to develop integrated models for design and operation of those strategies. Several integrated model [25–27] have been established to combine the design of lane markings and signal timings for isolated signalized intersections. It was shown that substantial improvement in the intersection performance can be achieved by using the integrated model. In the network level, the benefit of integrated design and operation should be even more significant as there are more combinations of decisions and flexibility to accommodate different traffic flow patterns. However, only limited studies have been done regarding network enhancement with lane reorganization and traffic control strategies optimized in a unified framework. Wong and Yang [28] first developed a network reserve capacity model in a signalized network. Then, some studies have developed models for the integrated design of signal settings with network routing decisions [29, 30]. Except for these deterministic network design problems, a capacity–reliability index is introduced to measure the probability that all of the network links are operated below their capacities when serving different traffic patterns deviating from the average condition [31]. Then the models for the reliability-based network design problem are proposed [32], examined [33], and modified [34]. However, the lane reorganization strategies were not considered.

This paper aims to develop a lane-based optimization model, in which signal timing optimization and lane re-configuration are integrated in a unified framework, to select the most appropriate combination of traffic management strategies to enhance the network capacity. The rest of the paper is organized as follows. In Section 2, network representation and notations adopted in this paper are described. The optimization model is proposed in Section 3. Section 4 develops the heuristic to solve the model. Performance of the integrated model is evaluated through numerical analysis in Section 5. Findings and concluding remarks are made in the end.

DOI: 10.1002/atr

2. NETWORK REPRESENTATION

As illustrated in Figure 1, the target network $\mathcal{G} = (\mathcal{N}, \mathcal{S})$ consists of a set of intersections denoted by $\mathcal{N}$, $r \in \mathcal{N}$ and a set of links joining intersections denoted by $\mathcal{S}$, $a = (r, r') \in \mathcal{S}$. Each intersection r consists of a set of legs denoted by $\mathcal{A}_r$, $i \in \mathcal{A}_r$. And each leg i consists of a set of turning arcs denoted by $\mathcal{T}_i$, $w \in \mathcal{T}_i$, and a set of lanes denoted by $\mathcal{L}_i$, $k \in \mathcal{L}_i$. A pair of two directional links between two intersections r and r' can be defined as a segment, denoted by (a, a') with $a = (r, r')$ and $a' = (r', r)$.

For any lane $k \in \mathcal{L}_i$, denote x_{riwk} as the permission of arc w on lane k in leg i at intersection r. Then, turning restriction can be easily realized by setting the prohibited turning arc not permitted in any lanes in the leg. For any link $a \in \mathcal{S}$, denote n_a be the number of lanes on the link, $n_{a'}$ be the number of lanes on the link of opposing direction, and $n_{aa'}$ be the total number of lanes in both directions. Therefore, lane reversal and one-way street strategy can be realized by deciding the values of n_a and $n_{a'}$. A set of auxiliary binary variables δ_{riw} and δ_a are used to represent the permission of arc w on leg i at intersection r and on segment a, respectively (1—Yes, 0—No). Figure 2 illustrates an example network operated with different type of traffic management strategies.

Let $\mathcal{O} \subseteq \mathcal{N}$ represent the set of demand origins, $\mathcal{D} \subseteq \mathcal{N}$ represent the set of demand destinations, and (o, d) represent an OD pair with $o \in \mathcal{O}$, $d \in \mathcal{D}$. Let $Q_{o,d}$ be the traffic demand between (o, d), $q_{o,d}$ be the scaled traffic demand between (o, d), and $\mathcal{Z}_{o,d}$ represent the set of routes between (o, d). For any route $z \in \mathcal{Z}_{o,d}$, it may include a sequence of links and turning arcs. The binary variables $\delta_{o,d}^{az}$ and $\delta_{o,d}^{wz}$ are used to represent whether a route z between (o, d) traverses link a or turning arc w, respectively (1—Yes, 0—No). The scaled traffic demand on route z between (o, d) is denoted by $q_{o,d}^{z}$.

3. THE OPTIMIZATION MODEL

3.1. Notations

To facilitate the model presentation, notations and parameters used hereafter are listed in Table I.

3.2. The upper-level problem

The proposed model aims to maximize the reserve capacity for the given network. Reserve capacity is a commonly used performance indicator for a signal-controlled system [35, 36]. By adopting the commonly used assumption that the proportions of the traffic demand remain constant, maximizing the reserve capacity is equivalent to maximizing the common flow multiplier [26, 27], μ, given by:

$$\max \mu. \tag{1}$$

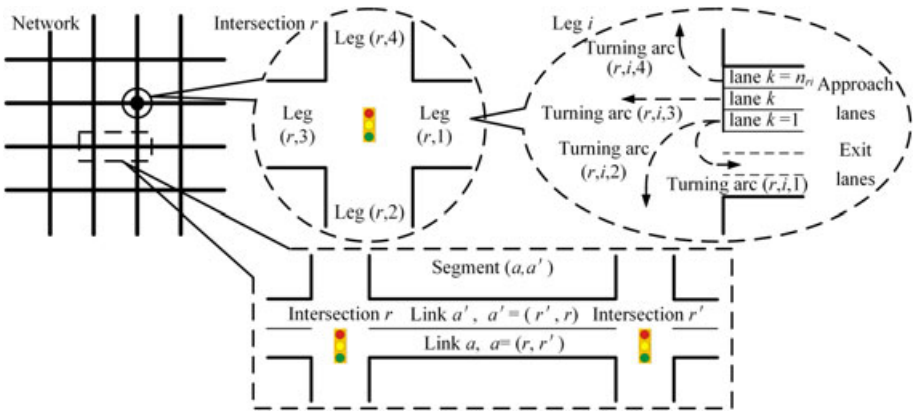

Figure 1. Example network representation.

DOI: 10.1002/atr

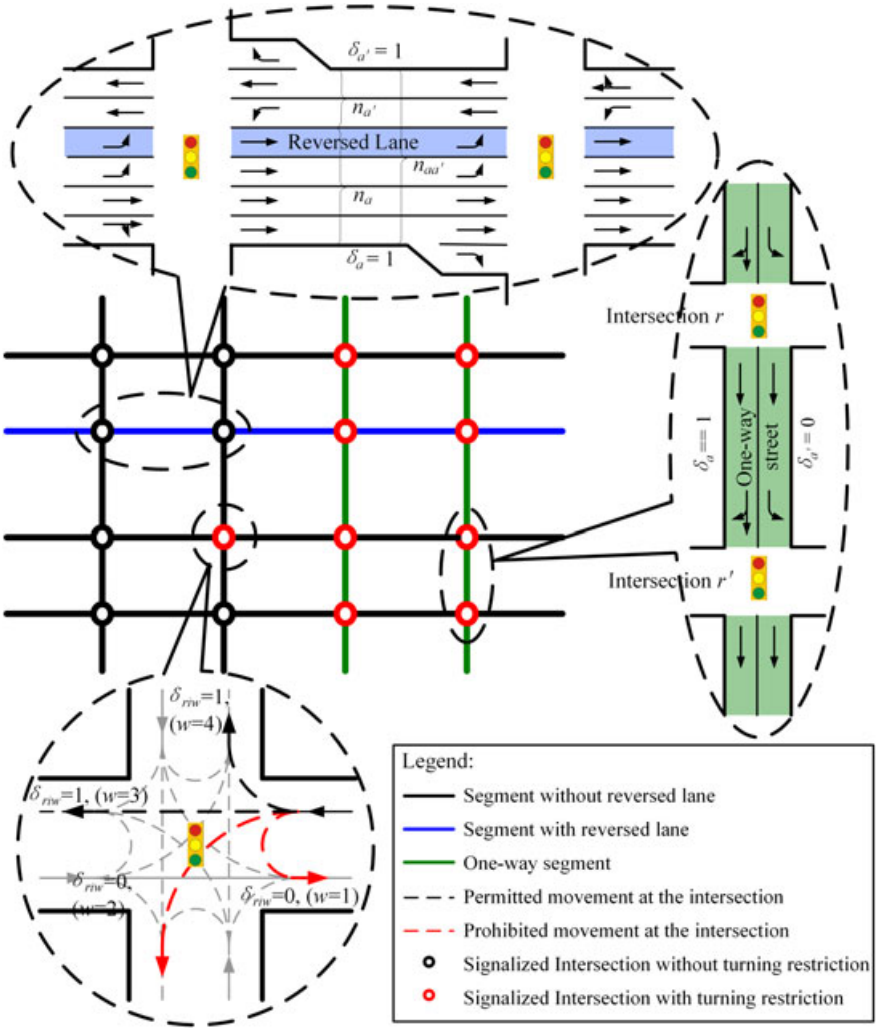

Figure 2. Traffic management strategies in a network.

The optimization problem should include the flow conservation constraints,

$$\mu Q_{o,d} = q_{o,d}, \quad \forall o \in \mathcal{O};\ d \in \mathcal{D} \tag{2}$$

$$q_{riw} = \sum_{k=1}^{n_{ri}} q_{riwk}, \quad \forall w \in \mathcal{T}_i;\ i \in \mathcal{A}_r;\ r \in \mathcal{N} \tag{3}$$

the lane assignment constraints,

$$n_{aa'} = n_a + n_{a'}, \quad \forall a = (r, r') \in \mathcal{S} \tag{4}$$

$$n_{ri}^s = n_{ri} + n_a, \quad \forall i \in \mathcal{A}_r;\ r \in \mathcal{N};\ a = (r, r') \in \mathcal{S};\ (ri, a) \in \mathcal{C} \tag{5}$$

$$\sum_{w \in \mathcal{T}_i} x_{riwk} \geq 1, \quad \forall k \in \mathcal{L}_i;\ i \in \mathcal{A}_r;\ r \in \mathcal{N} \tag{6}$$

DOI: 10.1002/atr

Table I. Notations of key model parameters and variables.

Network representation	
$\mathcal{N}$	Set of signalized intersections
$r \in \mathcal{N}$	Index of signalized intersections
$\mathcal{S}$	Set of links
$a, a' \in \mathcal{S}$	Index of links, link a' is the opposing direction of link a
$\mathcal{A}_r$	Set of legs in intersection r
$i \in \mathcal{A}_r$	Index of intersection legs, $i=1$ for east leg, $i=2$ for south leg, $i=3$ for west leg, and $i=4$ for north leg
$\mathcal{C}$	Set of legs and their connected links at intersection r
$\mathcal{T}$	Set of all turning arcs in the network
$\mathcal{T}_i$	Set of turning arcs in leg i
$\mathscr{R}$	Set of turning arcs and their receiving links at intersection r
$w \in \mathcal{T}_i$	Index of turning arcs in leg i, $w=1$ for U-turn, $w=2$ for left-turn, $w=3$ for through movement, and $w=4$ for right-turn
$\mathscr{L}_i$	Set of lanes in leg i
k	Index of lanes, numbering from the left-most lane
$\mathcal{O} \subseteq \mathcal{N}$	Set of demand origins
$\mathcal{D} \subseteq \mathcal{N}$	Set of demand destinations
(o, d)	An OD pair
$\mathcal{Z}_{o,d}$	Set of routes between (o, d)
$z \in \mathcal{Z}_{o,d}$	Index of routes
Parameters	
n^s_{ri}	Total number of lanes in both directions in leg i at intersection r
$n_{aa'}$	Total number of lanes in both directions of the segment (a, a')
$Q_{o,d}$	Traffic demand between (o, d), veh/h
E_{riw}	Numerical factor to convert vehicular flow of arc w on leg i at intersection r into through car unit
s_{rik}	Saturation flow rate of lane k in leg i at intersection r, veh/h
ds_{max}	Maximum acceptable degree of saturation
C_{min}, C_{max}	Minimum and maximum cycle length, s
$I_{r(iw,jw')}$	Clearance time for a pair of conflicting traffic turning arcs at intersection r, s
t^0_a	Free flow travel time at road section link a, s
t^0_{riw}	Free flow travel time at turning arc w in leg i at intersection r, s
k_a, b_a, k_w, b_w	Parameters in the BPR-form function
M	A large positive constant, it is set to be 10^9 in the numerical example
Decision variables	
μ	Common flow multiplier for the intersection group
x_{riwk}	A binary variable indicating the permission of arc w on lane k in leg i at intersection r
n_{ri}	Number of approach lanes
n_a	Number of lanes on link a
$q^z_{o,d}$	Scaled traffic demand on route z between (o, d), veh/h
q_{riwk}	Assigned flow of turning arc w on lane k in leg i at intersection r, veh/h
$\delta^{az}_{o,d}$	A binary variable showing whether a route z between (o, d) traverses link a (1—Yes, 0—No)
$\delta^{wz}_{o,d}$	A binary variable showing whether a route z between (o, d) traverses turning arc w (1—Yes, 0—No)
ξ_r	Reciprocal of signal cycle length at intersection r, 1/s
y_{riw}	Start of green for turning arc w in leg i at intersection r
λ_{riw}	Green split for turning arc w in leg i at intersection r
$P_{r(iw,jw')}$	Order of signal phase for a pair of conflicting turning arcs at intersection r (1—turning arc (i, w) follows turning arc (j, w'), 0—turning arc (j, w') follows turning arc (i, w))
γ_{rik}	Flow ratio of lane k in leg i at intersection r
ds_a	Degree of saturation on link a
ds_{riw}	Degree of saturation on turning arc w in leg i at intersection r
Auxiliary variables	
$q_{o,d}$	Scaled traffic demand between (o, d), veh/h, which could be calculated by the common flow multiplier (μ) and the given traffic demand $Q_{o,d}$
δ_{riw}	Permission of arc w on leg i at intersection r (1—Yes, 0—No), which could be determined by the number of lanes permitted for the turning arcs (x_{riwk})

(*Continues*)

DOI: 10.1002/atr

Table . (Continued)

Network representation	
δ_a	Permission of arc w on leg i on segment a (1—Yes, 0—No), which could be determined by the number of lanes in the link (n_a)
q_{riw}	Assigned flow of turning arc w on leg i at intersection r, veh/h, which could be calculated by the flows of a turning arc on different lanes (q_{riwk})
Y_{rik}	Start of green for lane k on leg i at intersection r, which could be determined by the start of green for turning arc (y_{riw}) and the lane assignment scheme (x_{riwk})
Λ_{rik}	Green split for lane k on leg i at intersection r, which could be determined by the green split for turning arc (λ_{riw}) and the lane assignment scheme (x_{riwk})
N_{pr}	Number of phases at intersection r, which could be determined by the order of signal phase ($P_{r(iw,jw')}$) and the turning restriction scheme (δ_{riw})
L_r	Total lost time at intersection r, s, which could be determined by the Number of phases (N_{pr}) and the given clearance time ($I_{r(iw,jw')}$)

$$M\delta_{riw} \geq \sum_{k=1}^{n_{ri}} x_{riwk} \geq \delta_{riw}, \quad \forall w \in \mathcal{T}_i;\ i \in \mathcal{A}_r;\ r \in \mathcal{N} \tag{7}$$

$$M\delta_a \geq n_a \geq \delta_a, \quad \forall a \in \mathcal{S} \tag{8}$$

$$M\delta_a \geq \sum_{w \in \mathcal{T}_{i'}} \delta_{r'i'w} \geq \delta_a, \quad \forall a = \left(r, r'\right) \in \mathcal{S};\ i' \in \mathcal{A}_r;\ r' \in \mathcal{N} \tag{9}$$

$$M\delta_a \geq \sum_{(rjw,a) \in \mathscr{R}} \delta_{rjw} \geq \delta_a, \quad \forall a = \left(r, r'\right) \in \mathcal{S};\ w \in \mathcal{T}_j;\ j \in \mathcal{A}_r;\ r \in \mathcal{N} \tag{10}$$

$$n_a \geq \sum_{k=1}^{n_{ri}} x_{rjwk}, \quad \forall (rjw, a) \in \mathscr{R};\ a = \left(r, r'\right) \in \mathcal{S};\ w \in \mathcal{T}_j;\ j \in \mathcal{A}_r;\ r \in \mathcal{N} \tag{11}$$

$$1 - x_{riw(k+1)} \geq x_{riw'k}, \ \forall k \in \{1, \ldots, n_{ri} - 1\}, \ w \in \{1, 2, 3\}, \ w' \in \{w + 1, \ldots, 4\}, i \in \mathcal{A}_r, \ r \in \mathcal{N} \tag{12}$$

the signal timing constraints,

$$\frac{1}{C_{min}} \geq \xi_r \geq \frac{1}{C_{max}}, \quad \forall r \in \mathcal{N} \tag{13}$$

$$1 \geq y_{riw} \geq 0, \quad \forall w \in \mathcal{T}_i;\ i \in \mathcal{A}_r;\ r \in \mathcal{N} \tag{14}$$

$$1 \geq \lambda_{riw} \geq 0, \quad \forall w \in \mathcal{T}_i;\ i \in \mathcal{A}_r;\ r \in \mathcal{N} \tag{15}$$

$$M\delta_{riw} \geq \lambda_{riw} \geq -M\delta_{riw}, \quad \forall w \in \mathcal{T}_i;\ i \in \mathcal{A}_r;\ r \in \mathcal{N} \tag{16}$$

$$M(1 - x_{riwk}) \geq Y_{rik} - y_{riw} \geq -M(1 - x_{riwk}), \ \forall k \in \mathscr{S}_i;\ w \in \mathcal{T}_i;\ i \in \mathcal{A}_r;\ r \in \mathcal{N} \tag{17}$$

$$M(1 - x_{riwk}) \geq \Lambda_{rik} - \lambda_{riw} \geq -M(1 - x_{riwk}), \ \forall k \in \mathscr{S}_i;\ w \in \mathcal{T}_i;\ i \in \mathcal{A}_r;\ r \in \mathcal{N} \tag{18}$$

DOI: 10.1002/atr

$$P_{r(iw,jw')} + P_{r(jw',iw)} = 1, \quad \forall w \in \mathcal{T}_i; w' \in \mathcal{T}_j;\ i,j \in \mathcal{A}_r;\ r \in \mathcal{N} \tag{19}$$

$$y_{rjw'} + P_{r(iw,jw')} \geq y_{riw} + \lambda_{riw} + \delta_{riw} I_{r(iw,jw')} \xi_r, \quad \forall w \in \mathcal{T}_i; w' \in \mathcal{T}_j;\ i,j \in \mathcal{A}_r;\ r \in \mathcal{N} \tag{20}$$

the acceptable level-of-service constraints,

$$\gamma_{rik} = \frac{\sum_{w \in T_i} (q_{riwk} E_{riw})}{s_{rik}}, \quad \forall k \in \mathcal{S}_i;\ i \in \mathcal{A}_r;\ r \in \mathcal{N} \tag{21}$$

$$M\left(2 - x_{riwk} - x_{riw(k+1)}\right) \geq \gamma_{ri(k+1)} - \gamma_{rik} \geq -M\left(2 - x_{riwk} - x_{riw(k+1)}\right), \quad \forall k \in \mathcal{S}_i;\ w \in \mathcal{T}_i;\ i \in \mathcal{A}_r;\ r \in \mathcal{N} \tag{22}$$

$$ds_{\max} \Lambda_{rik} \geq \gamma_{rik}, \quad \forall k \in \mathcal{S}_i;\ i \in \mathcal{A}_r;\ r \in \mathcal{N} \tag{23}$$

$$ds_{\max} s_a n_a \geq q_a, \quad \forall a \in \mathcal{S} \tag{24}$$

and the non-negative constraints for all decision variables listed in section 3.1.

Constraint (2) obtains the scaled traffic demand matrix given the set of demand origins and destinations as an exogenous input. Constraint (3) indicates that the sum of the flows of a turning arc on different lanes should be equal to the total assigned flow of that turning arc.

Constraint (4) sets the total number of lanes in a segment, which adds the number of lanes on links of two directions. Constraint (5) sets the total number of lanes in a leg, which is equal to the sum of the number of approach and receiving lanes. Constraint (6) allows each lane to carry at least one turning or through movement. Constraint (7) sets the turning restriction strategy: if a turning arc at the intersection is prohibited, the number of lanes permitted for the prohibited turning arcs should be equal to 0; otherwise, the turning arc should be permitted in at least one lane. Constraint (8)–(10) sets the one-way street strategy: if the right-of-way of a link is prohibited, the number of lanes in the link should be set to 0, as illustrated by Constraint (8); all turning arcs in the approach connecting to the link should be prohibited, as indicated by Constraint (9); and all the turning arcs entering the link should also be prohibited, as indicated by Constraint (10). Constraint (11) sets that the number of lanes in a turning arc's corresponding receiving link should be at least as many as the number of lanes assigned to that turning arc to ensure safety and operational efficiency. Constraint (12) prevents internal conflicts among lanes in a leg.

Constraint (13) limits the common cycle length for the intersections in the network to be within the minimum and maximum cycle lengths. Instead of defining the cycle length directly as the control variable, its reciprocal is used to preserve the linearity in the mathematical formulation [26, 27]. Constraint (14) confines the start of the green to be within a fraction between 0 and 1 of the cycle length. Constraint (15) indicates that the green split of a turning arc is confined between 0 and 1 of the cycle length. Constraint (16) sets that the green split of a turning arc should be equal to 0 if the turning arc is prohibited. Constraints (17)–(18) define the lane signal timings. Constraint (19) sets the order of signal phase display for a pair of conflicting turning arcs at intersection r, which is governed by a successor function [37]. Constraint (20) limits the start of greens for any pair of conflicting turning arcs considering the minimum clearance time and turning arc prohibition.

Constraint (21) obtains the flow ratio. Constraint (22) sets the flow ratios on a pair of adjacent approach lanes to be identical if they share a common lane marking. Constraints (23) and (24) limit the degree of saturation for each approach lane and each link to be no more than the maximum limit to ensure acceptable level of service.

DOI: 10.1002/atr

3.3. The lower-level problem

The lower-level problem specifies the routing assignment of the traffic demand under the assumption that the drivers will route in the network without violating the turning restrictions and signal control constraints. The network flow distribution will therefore reflect the drivers' route choice behaviors under a given network layout and signal timing scheme $\boldsymbol{\eta}=(\mathbf{n},\mathbf{x},\boldsymbol{\xi},\mathbf{Y},\boldsymbol{\Lambda},\mathbf{P})$ with $\mathbf{n}=(n_a|a\in\mathcal{S})$, $\mathbf{x}=(x_{riwk}|k\in\mathscr{S}_i;\ w\in\mathcal{T}_i;\ i\in\mathcal{A}_r;\ r\in\mathcal{N})$, $\boldsymbol{\xi}=(\xi_r|r\in\mathcal{N})$, $\mathbf{Y}=(Y_{rik}|k\in\mathscr{S}_i;\ i\in\mathcal{A}_r;\ r\in\mathcal{N})$, $\boldsymbol{\Lambda}=(\Lambda_{rik}|k\in\mathscr{S}_i;\ i\in\mathcal{A}_r;\ r\in\mathcal{N})$, and $\mathbf{P}=\left(P_{r(iw,jw')}\middle|w\in\mathcal{T}_i;w'\in\mathcal{T}_j;\ i,j\in\mathcal{A}_r;\ r\in\mathcal{N}\right)$. Because network enhancement is usually not a short-term event, we adopt the user equilibrium (UE) principle to capture the resulting network flow pattern in this model. Based on the UE principle, no driver could unilaterally decrease his/her transportation disutility by changing routes between a certain OD pair.

The disutility along a route could be expressed as the sum of disutilities along its comprising links and turning arcs, which is expressed by the travel times. As show in Equations (25) and (26), the BPR-form function is adopted to estimate the disutility on the link and turning arcs.

$$\mathbf{u}_a(\mathbf{q},\boldsymbol{\eta})=t_a^0\left[1+k_a(ds_a)^{b_a}\right],\ \ \forall a\in\mathcal{S} \tag{25}$$

$$\mathbf{u}_w(\mathbf{q},\boldsymbol{\eta})=t_{riw}^0\left[1+k_w(ds_{riw})^{b_w}\right],\ \ \forall w\in\mathcal{T}_i;\ i\in\mathcal{A}_r;\ r\in\mathcal{N} \tag{26}$$

Then, the UE problem can be formulated below [38], where $\mathbf{q}=(\mathbf{q_a},\mathbf{q_w})=\{(q_a,\ \forall a\in\mathcal{S})\cup(q_w,\ \forall w\in\mathcal{T})\}$ represents the flow pattern under the solution $\boldsymbol{\eta}$; $\mathbf{q_a}$ and $\mathbf{q_w}$ are the flow vectors of links and turning arcs, respectively; $\mathbf{q_a^*}$ and $\mathbf{q_w^*}$ represent the UE flow pattern. Note that the degree of saturation in Equation (23, 24) is equal to the traffic flow divided by the capacity of the link or arc. Therefore, the Equation (23, 24) and Equation (27–31) could be connected using traffic flow variables.

$$min\ \sum\nolimits_{a\in\mathcal{S}}\int_0^{q_a}u_a(x)dx+\sum\nolimits_{w\in\mathcal{T}}\int_0^{q_w}u_w(x)dx \tag{27}$$

$$s.t.\ \ q_{o,d}=\sum\nolimits_{z\in\mathcal{Z}_{o,d}}q_{o,d}^z,\ \ \forall o\in\mathcal{O};\ d\in\mathcal{D} \tag{28}$$

$$q_a,\ q_w\geq 0,\ \ \forall a\in\mathcal{S};\ w\in\mathcal{T} \tag{29}$$

$$q_a=\sum\nolimits_{o\in\mathcal{O}}\sum\nolimits_{d\in\mathcal{D}}\sum\nolimits_{z\in\mathcal{Z}_{o,d}}q_{o,d}^z\delta_{o,d}^{az},\ \ \forall a\in\mathcal{S} \tag{30}$$

$$q_w=\sum\nolimits_{o\in\mathcal{O}}\sum\nolimits_{d\in\mathcal{D}}\sum\nolimits_{z\in\mathcal{Z}_{o,d}}q_{o,d}^z\delta_{o,d}^{wz},\ \ \forall w\in\mathcal{T} \tag{31}$$

4. SOLUTION

The proposed optimization model has a bi-level structure with a mix-integer-non-linear-programming problem at the upper-level and a parametric variational inequality at the lower-level. It is therefore NP-hard and difficult to solve because of its non-convexity and non-differential characteristics. In this section, we developed a genetic algorithm (GA) based heuristic method to yield viable and approximate optimal solutions to the model in a reasonable time period. The procedure of the algorithm flow is illustrated in Figure 3. It is a double-cycle system to avoid the remaining local optima of GAs. The GA is the inner loop to find an available solution that satisfying the degree of saturation

DOI: 10.1002/atr

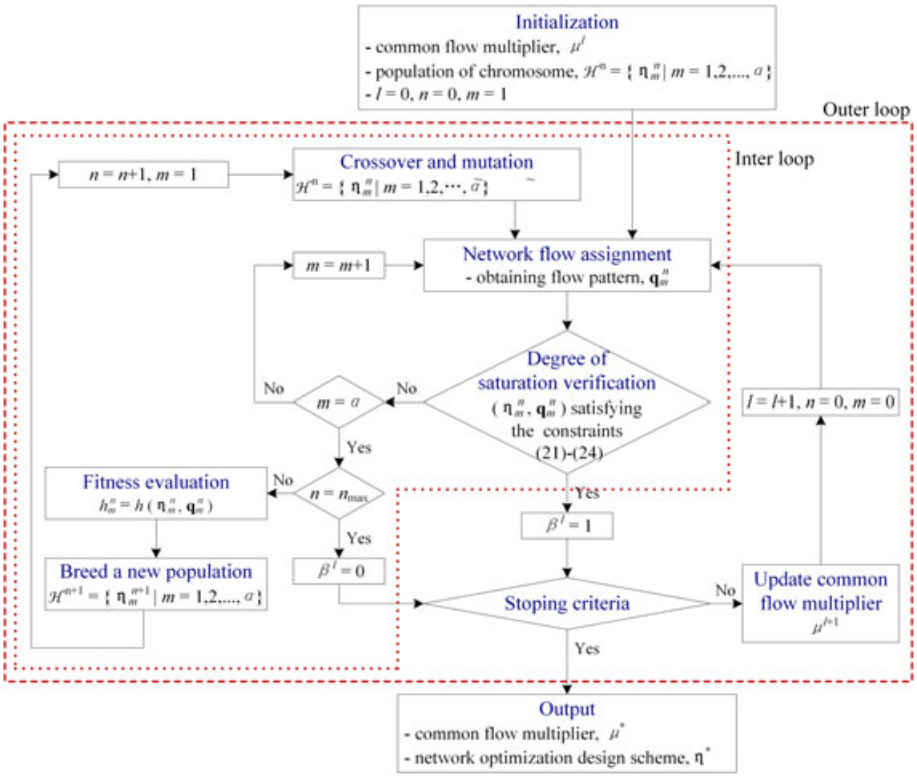

Figure 3. Procedure of the heuristic algorithm.

verification for a given common flow multiplier determined at the outer loop. The binary string of the solution is given as Figure 4.

Specifics on each module of the algorithm are illustrated as follows:

4.1. Coding of the GA

(1) The layout variables. According to Figure 4, the number of lanes on each odd link, n_a, and the random 0-1 variables to determine the permission of turning on each lane on each leg at each intersection, f_{riwk}, are generated. Then, the number of lanes on each even link could encoded as Equation (32). The number of approach lanes could encoded as Equation (33). The permission of turning w on lane k on leg i at intersection r used in the chromosome, x_{rijk}, could be encoded as Equation (34–38). Additionally, the permission of arc w on leg i at intersection r, δ_{riw}, and the permission of arc w on leg i on segment a, δ_a, could be encoded as Equation (39) and (40), respectively.

$$n_{a'} = n_{aa'} - n_a, \quad \forall a \in \mathcal{S} \tag{32}$$

$$n_{ri} = n_{ri}^s - n_a, \quad \forall i \in \mathcal{A}_r;\ r \in \mathcal{N};\ a = (r, r') \in \mathcal{S};\ (ri, a) \in \mathcal{C} \tag{33}$$

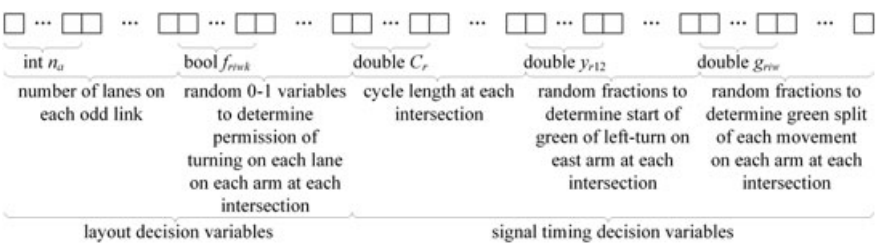

Figure 4. Binary string of the solution.

DOI: 10.1002/atr

$$x_{riw1} = f_{riw1}\left\lceil\frac{n_{a1}}{M}\right\rceil\left\lceil\frac{n_{a2}}{M}\right\rceil,\ \forall(riw,a2)\in\mathscr{R};\ a1 = (r,r')\in\mathcal{S};\ w\in\mathcal{T}_j;\ i\in\mathcal{A}_r;\ r\in\mathcal{N} \tag{34}$$

$$\begin{aligned} x_{ri1(k+1)} &= f_{ri1(k+1)}(1-x_{ri2k})(1-x_{ri3k})(1-x_{ri4k})\left\lceil\frac{n_{a1}}{M}\right\rceil\left\lfloor\frac{n_{a2}-\sum_{k=1}^{k}x_{ri1k}}{M}\right\rfloor,\ \forall(ri1,a2)\in\mathscr{R};\ a1 \\ &= (r,r')\in\mathcal{S};\ k\in\{1,\ldots,n_{ri}-1\};\ i\in\mathcal{A}_r;\ r\in\mathcal{N} \end{aligned} \tag{35}$$

$$\begin{aligned} x_{ri2(k+1)} &= f_{ri2(k+1)}(1-x_{ri3k})(1-x_{ri4k})\frac{n_{a1}}{M}\frac{n_{a2}-\sum_{k=1}^{k}x_{ri2k}}{M}\ \forall(ri2,a2)\in\mathscr{R};\ a1 \\ &= (r,r')\in\mathcal{S};\ k\in\{1,\ldots,n_{ri}-1\};\ i\in\mathcal{A}_r;\ r\in\mathcal{N} \end{aligned} \tag{36}$$

$$\begin{aligned} x_{ri3(k+1)} &= f_{ri3(k+1)}(1-x_{ri4k})\left\lceil\frac{n_{a1}}{M}\right\rceil\left\lfloor\frac{n_{a2}-\sum_{k=1}^{k}x_{ri3k}}{M}\right\rfloor\ \forall(ri3,a2)\in\mathscr{R};\ a1 \\ &= (r,r')\in\mathcal{S};\ k\in\{1,\ldots,n_{ri}-1\};\ i\in\mathcal{A}_r;\ r\in\mathcal{N} \end{aligned} \tag{37}$$

$$\begin{aligned} x_{ri4(k+1)} &= f_{ri4(k+1)}\left\lceil\frac{n_{a1}}{M}\right\rceil\left\lfloor\frac{n_{a2}-\sum_{k=1}^{k}x_{ri4k}}{M}\right\rfloor\ \forall(ri4,a2)\in\mathscr{R};\ a1 \\ &= (r,r')\in\mathcal{S};\ k\in\{1,\ldots,n_{ri}-1\};\ i\in\mathcal{A}_r;\ r\in\mathcal{N} \end{aligned} \tag{38}$$

$$\delta_{riw} = \left\lceil\frac{\sum_{k=1}^{n_{ri}}x_{riwk}}{M}\right\rceil,\ \forall w\in\mathcal{T}_i;\ i\in\mathcal{A}_r;\ r\in\mathcal{N} \tag{39}$$

$$\delta_a = \frac{n_a}{M},\ \forall a\in\mathcal{S} \tag{40}$$

(2) The signal control variables. According to Figure 4, cycle length at each intersection, C_r, start of green of each turning arc on each leg at each intersection, y_{riw}, and the random fractions to determine the green split of each turning arc on each leg at each intersection, g_{rik}, are generated. Then, the phase plan at each intersection could be encoded as Equation (41, 42). The total lost time could be encoded as Equation (43, 44). The green split of each turning arc on each leg at each intersection, x_{rijk}, could be encoded as Equation (45–66).

$$P_{ri} = min\left(max\left(\begin{array}{c}\sum_{i=1,3}\sum_{k=1}^{n_{ri}}(x_{ri1k}x_{ri3k}),\sum_{i=1,3}\sum_{k=1}^{n_{ri}}(x_{ri1k}x_{ri4k}),\\ \sum_{i=1,3}\sum_{k=1}^{n_{ri}}(x_{ri2k}x_{ri3k}),\sum_{i=1,3}\sum_{k=1}^{n_{ri}}(x_{ri2k}x_{ri4k})\end{array}\right),0\right),\ \forall r\in\mathcal{N};i\in\{1,3\} \tag{41}$$

$$P_{ri} = min\left(max\left(\begin{array}{c}\sum_{i=2,4}\sum_{k=1}^{n_{ri}}(x_{ri1k}x_{ri3k}),\sum_{i=2,4}\sum_{k=1}^{n_{ri}}(x_{ri1k}x_{ri4k}),\\ \sum_{i=2,4}\sum_{k=1}^{n_{ri}}(x_{ri2k}x_{ri3k}),\sum_{i=2,4}\sum_{k=1}^{n_{ri}}(x_{ri2k}x_{ri4k})\end{array}\right),0\right),\ \forall r\in\mathcal{N};i\in\{2,4\} \tag{42}$$

$$L_r = \begin{cases} P_r\dfrac{\omega}{C_r}, & N_{pr}\geq 2 \\ 0, & N_{pr}\leq 1 \end{cases},\ \forall r\in\mathcal{N} \tag{43}$$

DOI: 10.1002/atr

$$N_{pr} = P_{r1}\sum_{i=1,3}\left\lceil\frac{\sum_{w=1}^{4}\delta_{riw}}{M}\right\rceil + (1-P_{r1})max\begin{pmatrix} min(\,\delta_{r11}+\delta_{r12},1)+min(\,\delta_{r33}+\delta_{r34},1),\\ min(\,\delta_{r13}+\delta_{r14},1)+min(\,\delta_{r31}+\delta_{r32},1)\end{pmatrix}+$$

$$P_{r2}\sum_{i=2,4}\left\lceil\frac{\sum_{w=1}^{4}\delta_{riw}}{M}\right\rceil + (1-P_{r2})max\begin{pmatrix} min(\,\delta_{r21}+\delta_{r22},1)+min(\,\delta_{r43}+\delta_{r44},1)\,,\\ min(\,\delta_{r23}+\delta_{r24},1)+min(\delta_{r41}+\delta_{r42},1)\end{pmatrix}, \forall r\in\mathcal{N} \quad (44)$$

$$\lambda_{r1} = max\left(g_{r1}, 1-\left\lceil\frac{\sum_{i=2,4}\sum_{w=1}^{4}\delta_{riw}}{M}\right\rceil\right)\left\lceil\frac{\sum_{i=1,3}\sum_{w=1}^{4}\delta_{riw}}{M}\right\rceil(1-L_r),\ \ \forall r\in\mathcal{N} \quad (45)$$

$$\lambda_{r2} = (1-L_r-\lambda_{r1}),\ \ \forall r\in\mathcal{N} \quad (46)$$

$$\lambda_{r1w} = \lambda_{r1}g_{r11}\delta_{r1w},\quad \forall P_{r1}=1;\ \ r\in\mathcal{N};\ w\in\mathcal{T}_i \quad (47)$$

$$\lambda_{r3w} = (\lambda_{r1}-max(\lambda_{r11},\lambda_{r12},\lambda_{r13},\lambda_{r14}))\delta_{r3w},\quad \forall P_{r1}=1;\ \ r\in\mathcal{N};\ w\in\mathcal{T}_i \quad (48)$$

$$\lambda_{r11} = \lambda_{r1}max\left(g_{r11}, 1-\left\lceil\frac{\sum_{w=3}^{4}\delta_{r3w}}{M}\right\rceil\right)\delta_{r11},\quad \forall P_{r1}=0;\ \ r\in\mathcal{N} \quad (49)$$

$$\lambda_{r12} = \lambda_{r1}max\left(g_{r11}, 1-\left\lceil\frac{\sum_{w=3}^{4}\delta_{r3w}}{M}\right\rceil\right)\delta_{r12},\quad \forall P_{r1}=0;\ \ r\in\mathcal{N} \quad (50)$$

$$\lambda_{r13} = \lambda_{r1}max\left(g_{r13}, 1-\left\lceil\frac{\sum_{w=1}^{2}\delta_{r3w}}{M}\right\rceil\right)\delta_{r13},\quad \forall P_{r1}=0;\ \ r\in\mathcal{N} \quad (51)$$

$$\lambda_{r14} = \lambda_{r1}max\left(g_{r13}, 1-\left\lceil\frac{\sum_{w=1}^{2}\delta_{r3w}}{M}\right\rceil\right)\delta_{r14},\quad \forall P_{r1}=0;\ \ r\in\mathcal{N} \quad (52)$$

$$\lambda_{r31} = \delta_{r31}(\lambda_{r1}-max(\lambda_{r13},\lambda_{r14})),\quad \forall P_{r1}=0;\ \ r\in\mathcal{N} \quad (53)$$

$$\lambda_{r32} = \delta_{r32}(\lambda_{r1}-max(\lambda_{r13},\lambda_{r14})),\quad \forall P_{r1}=0;\ \ r\in\mathcal{N} \quad (54)$$

$$\lambda_{r33} = \delta_{r33}(\lambda_{r1}-max(\lambda_{r11},\lambda_{r12})),\quad \forall P_{r1}=0;\ \ r\in\mathcal{N} \quad (55)$$

$$\lambda_{r34} = \delta_{r34}(\lambda_{r1}-max(\lambda_{r11},\lambda_{r12})),\quad \forall P_{r1}=0;\ \ r\in\mathcal{N} \quad (56)$$

$$\lambda_{r2w} = \lambda_{r2}g_{r21}\delta_{r2w},\quad \forall P_{r2}=1;\ \ r\in\mathcal{N};\ w\in\mathcal{T}_i \quad (57)$$

DOI: 10.1002/atr

$$\lambda_{r4w} = \delta_{r4w}(\lambda_{r2} - max(\lambda_{r21}, \lambda_{r22}, \lambda_{r23}, \lambda_{r24})), \quad \forall P_{r2} = 1; \ r \in \mathcal{N}; \ w \in \mathcal{T}_i \tag{58}$$

$$\lambda_{r21} = \lambda_{r2} max\left(g_{r21}, 1 - \left\lceil \frac{\sum_{w=3}^{4} \delta_{r4w}}{M} \right\rceil\right)\delta_{r21}, \quad \forall P_{r2} = 0; \ r \in \mathcal{N} \tag{59}$$

$$\lambda_{r22} = \lambda_{r2} max\left(g_{r21}, 1 - \left\lceil \frac{\sum_{w=3}^{4} \delta_{r4w}}{M} \right\rceil\right)\delta_{r22}, \quad \forall P_{r2} = 0; \ r \in \mathcal{N} \tag{60}$$

$$\lambda_{r23} = \lambda_{r2} max\left(g_{r23}, 1 - \left\lceil \frac{\sum_{w=1}^{2} \delta_{r4w}}{M} \right\rceil\right)\delta_{r23}, \quad \forall P_{r2} = 0; \ r \in \mathcal{N} \tag{61}$$

$$\lambda_{r24} = \lambda_{r2} max\left(g_{r23}, 1 - \left\lceil \frac{\sum_{w=1}^{2} \delta_{r4w}}{M} \right\rceil\right)\delta_{r24}, \quad \forall P_{r2} = 0; \ r \in \mathcal{N} \tag{62}$$

$$\lambda_{r41} = \lambda_{r41}(\lambda_{r2} - max(\lambda_{r23}, \lambda_{r24})), \quad \forall P_{r2} = 0; \ r \in \mathcal{N} \tag{63}$$

$$\lambda_{r42} = \lambda_{r42}(\lambda_{r2} - max(\lambda_{r23}, \lambda_{r24})), \quad \forall P_{r2} = 0; \ r \in \mathcal{N} \tag{64}$$

$$\lambda_{r43} = \delta_{r43}(\lambda_{r2} - max(\lambda_{r21}, \lambda_{r22})), \quad \forall P_{r2} = 0; \ r \in \mathcal{N} \tag{65}$$

$$\lambda_{r44} = \delta_{r44}(\lambda_{r2} - max(\lambda_{r21}, \lambda_{r22})), \quad \forall P_{r2} = 0; \ r \in \mathcal{N} \tag{66}$$

4.2. Initialization

An initial common flow multiplier μ^l ($l=0$) and a population consisting of α distinct chromosomes, denoted by $\mathscr{H}^n = \{\boldsymbol{\eta}_m^n | m = 1, 2, \ldots, \alpha\}$, are generated satisfying constraints (2)–(20), where l represents the index of iteration; n represents the index of GA generation; m represents the index of chromosome; $\boldsymbol{\eta}_m^n$ is a binary string representing chromosome m at generation n.

4.3. Crossover and mutation

One-point crossover and mutation operations are performed on the chromosomes selected from $\mathscr{H}^n$ to generate new solution populations, and $\mathscr{H}^n$ is the set of all resulting offspring chromosomes that satisfy constraint (2)-(20).

4.4. Network flow assignment

The Frank–Wolfe algorithm is used to obtain the UE flow pattern $\mathbf{q}_m^n$ corresponding to the design decision $\boldsymbol{\eta}_m^n$ [39].

DOI: 10.1002/atr

4.5. Degree of saturation verification

Although each chromosome in the population is generated satisfying constraints (2)–(20), the degree of saturation constraints may still be violated because the traffic flows on links and turning arcs cannot be obtained before finishing the network flow assignment step. To deal with this problem, the feasibility verification step is designed. For the solution $\left(\boldsymbol{\eta}_m^n, \mathbf{q}_m^n\right)$, if the degree of saturation constraints (21)–(24) are satisfied, the algorithm will go to the step of stopping criteria check directly; otherwise, the algorithm will continue searching the solutions.

4.6. Fitness evaluation

Given $\boldsymbol{\eta}_m^n$ and $\mathbf{q}_m^n$ $(m = 1, 2, \ldots, \alpha)$, the evaluation function of chromosome m at generation n, $h_m^n = h\left(\boldsymbol{\eta}_m^n, \mathbf{q}_m^n\right)$, can be calculated by Equation (67). Then the fitness of each chromosome can be then computed by normalizing its evaluation value with Equation (68).

$$h(\mathbf{v}, \boldsymbol{\eta}) = \sum_{r\in\mathcal{N}}\sum_{i\in\mathcal{A}_r}\sum_{w\in\mathcal{T}_i}\left(\max(ds_{riw} - ds_{\max}, 0)\right) + \sum_{a\in\mathcal{S}}\left(\max(ds_a - ds_{\max}, 0)\right) \tag{67}$$

$$\tilde{h}_m^n(\mathbf{v}, \boldsymbol{\eta}) = \frac{h_{\max}^n - h\left(\boldsymbol{\eta}_m^n, \mathbf{v}_m^n\right) + \varepsilon}{h_{\max}^n - h_{\min}^n + \varepsilon} \tag{68}$$

where $h(\mathbf{v}, \boldsymbol{\eta})$ is the evaluation function; $h_{\max}^n$ and $h_{\min}^n$ denote the maximum and minimum evaluation function values at generation n, respectively; ε is set to be 0.1 which functions to prevent Equation (68) from zero division and adjust the selection behavior between fitness proportional selection and pure random selection [40].

4.7. Breed a new populations

Generate the new population $\mathscr{H}^{n+1}$ of size α by using a binary tournament selection method [40] according to the fitness of each chromosome calculated with Equation (68).

4.8. Update the common flow multiplier

The common flow multiplier is adjusted according to the dichotomy search [41], given by Equation (69). The dichotomic principle search is a search algorithm that operates by selecting between two distinct alternatives (dichotomies) at each step. In each step, the algorithm compares the search key value with the key value of the middle element of the array. If the keys match, then a matching element has been found and its index, or position, is returned. Otherwise, if the search key is less than the middle element's key, then the algorithm repeats its action on the sub-array to the left of the middle element or, if the search key is greater, on the sub-array to the right.

$$\mu^{l+1} = \mu^l + \rho\prod_{l=0}^{l}\beta^l + \frac{\mu^l - \mu^{l-1}}{2}\left(2\beta^l - 1\right)\left(2\beta^{l-1} - 1\right)\left(1 - \prod_{l=0}^{l}\beta^l\right) \tag{69}$$

where β^l is a binary indicator showing whether a solution is found at iteration l (1—Yes, 0—No); ρ is the searching step size.

4.9. Stopping criteria

The algorithm would not stop unless the difference between the common flow multipliers of two adjacent iterations l and $l-1$ is less than a threshold ϵ:

$$\left|\mu^l - \mu^{l-1}\right| \le \epsilon \tag{70}$$

DOI: 10.1002/atr

5. A NUMERICAL EXAMPLE

In this section, a network (see Figure 5) with 40 segments (80 links) and 32 nodes (16 nodes are demand origins and destinations) is employed to test the proposed model. Each link in the network has three lanes, and all intersections are four-leg signalized intersections.

Traffic demand of all OD pairs is set to be 100vph; length of each link is 600 m; ds_{max} is set to be 0.9; C_{min} and C_{max} are set to be 60s and 120 s; s_{ik} is set to 1800veh/h/ln for all lanes; clearance time for any pair of conflicting turning arcs is set to be 4 s; the arbitrary large positive constant number, M, is set to be 10^9. In the BPR function, k_a, b_a, k_w, and b_w are set to be 0.15, 4.0, 20, and 3.5, respectively. In the GA, the crossover probability is set to be 0.25, mutation probability is set to be 0.01, the maximum number of GA generations n_{max} is set to be 100, and the population size α is set to be 50. The initial common flow multiplier, μ^0, is set to be 0.5. The searching step size, ρ, is set to be 0.2. The stopping threshold, ϵ, is set to be 0.001.

Performance of the proposed optimization model (Strategy 1) is compared with other three strategies:

Strategy 2: Conventional design (lane marking and signal timing only, no reversible lanes or turning restrictions)
Strategy 3: Left-turn restriction system only
Strategy 4: One-way street system only

All the models are solved on an Intel(R) Core(TM) i5 2.30 GHz processor and 4.0 GB RAM, running under Windows. The computing times are less than 300 min.

Figure 6 illustrates the solution convergence curves of the outer loop in Figure 3. Figure 7 shows an example of the GA convergence statistics in a step of the outer loop. In order to examine the validity and robustness of GA to solve the proposed model, this study solves the proposed optimization model (Strategy 1) for 40 times and the statistical measures of GA convergence and survival rates are summarized in Tables II and III, respectively. Table IV shows an example of a traffic assignment result to validate that the lower-level results satisfy the UE principle.

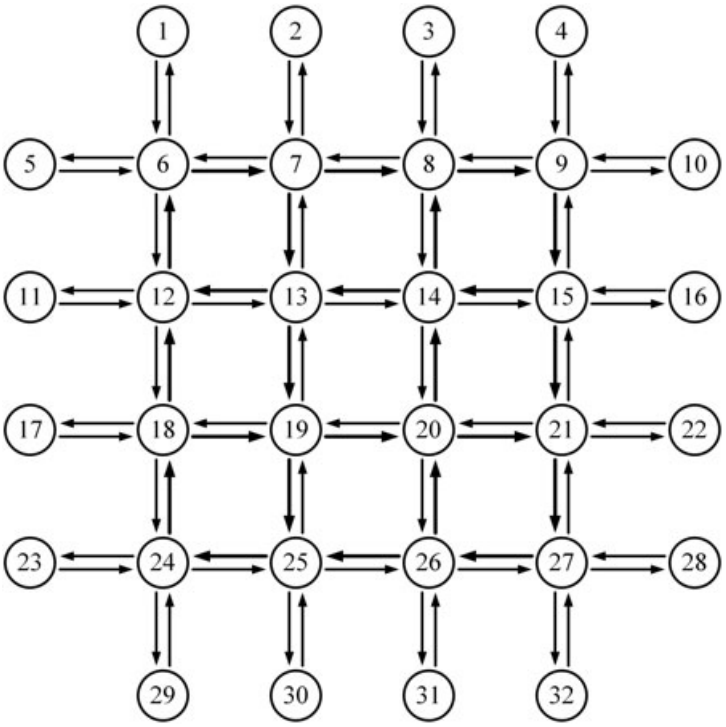

Figure 5. The test network.

DOI: 10.1002/atr

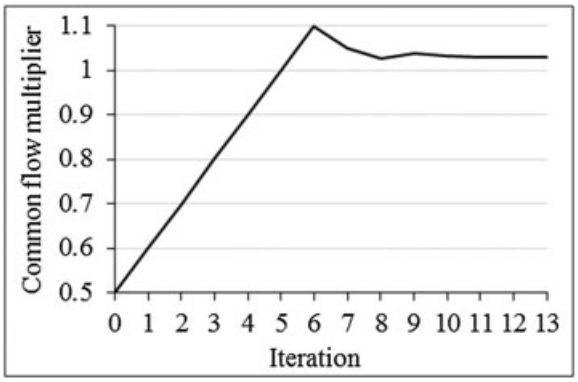

Figure 6. Solution convergence curves for Strategy 1.

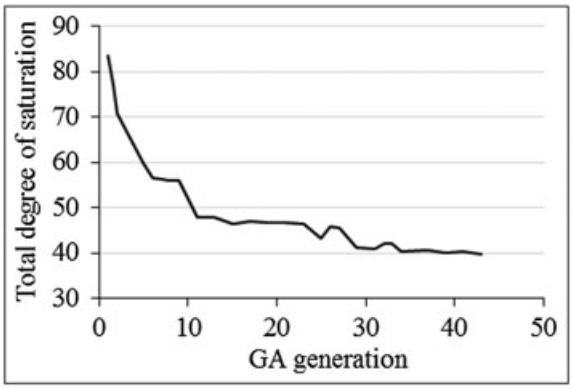

Figure 7. Example of GA convergence curve in a step of outer loop.

Table II. Statistics of number of generations for GA to convergence.

# of GA runs	# of generations to converge			
40	Mean	Minimum	Maximum	Std. deviation
	613	564	682	27.41

Table III. Statistics of survival rates.

Sample size	Mean	Minimum	Maximum	Std. deviation
24 530	0.479	0.28	0.66	0.053

Table IV. Traffic assignment results of two O-D pairs under two candidate strategies.

OD pair	Strategy	No. of route	Routes	Volume (veh/h)	Travel time (s)
node 2 to node 22	Strategy 2	1	2-7-13-14-15-21-22	15.73	1529.47
		2	2-7-13-14-20-21-22	18.85	1529.19
		3	2-7-13-19-20-21-22	35.11	1529.18
		4	2-7-8-9-15-21-22	2.50	1530.07
		5	2-7-8-14-20-21-22	18.54	1529.56
		6	2-7-8-14-15-21-22	9.27	1529.84

DOI: 10.1002/atr

Table V. Optimized signal timing plans from the proposed model (Strategy 1).

	Phase 1		Phase 2		Phase 3	
Intersection	Turning arcs	Duration of green (s)	Turning arcs	Duration of green (s)	Turning arcs	Duration of green (s)
6	EB-T, SB-L + R	39.55	NB-L + T + R	72.45	—	—
7	EB-L + T + R	72.44	SB-L + T	39.56	—	—
8	EB-L + T	22.81	NB-T + R	47.07	SB-L	38.12
9	EB-L + T + R	72.45	WB-L + R, SB-T	39.55	—	—
12	WB-T + R	47.07	EB-L	38.12	NB-L + T	22.81
13	WB-L + T	62.13	SB-T + R	49.87	—	—
14	WB-T + R	49.87	NB-L + T	62.13	—	—
15	WB-L + T	39.56	SB-L + T + R	72.44	—	—
18	EB-L + T	39.56	NB-L + T + R	72.44	—	—
19	EB-T + R	49.87	SB-L + T	62.13	—	—
20	EB-L + T	62.13	NB-T + R	49.87	—	—
21	WB-L	38.12	EB-T + R	47.07	SB-L + T	22.81
24	WB-L + T + R	72.45	EB-L + R, NB-T	39.55	—	—
25	WB-L + T	22.81	NB-L	38.12	SB-T + R	47.07
26	WB-L + T + R	72.44	NB-L + T	39.56	—	—
27	WB-T, NB-L + R	39.55	SB-L + T + R	72.45	—	—

Note: L, T, and R represent left-turn, through movement, and right-turn, respectively.

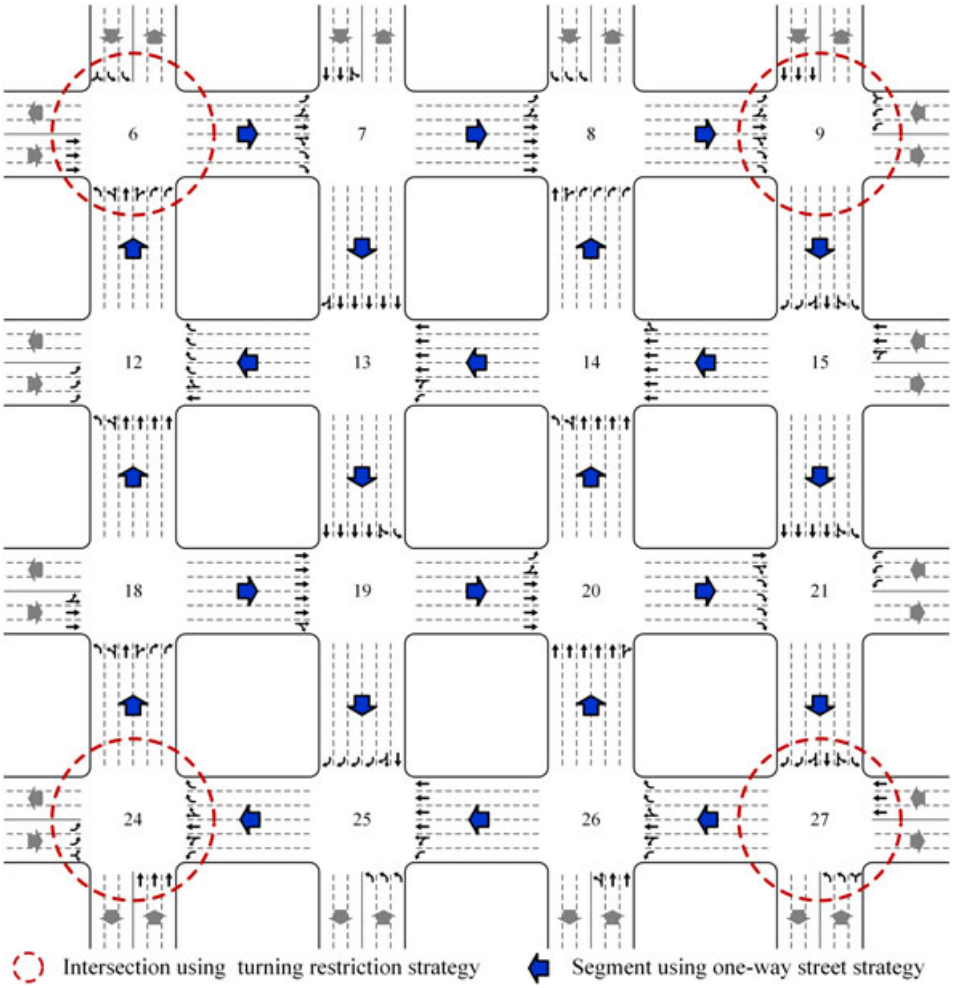

Figure 8. Optimized plans (Strategy 1).

DOI: 10.1002/atr

Table V illustrates the optimized signal timings for Strategy 1 and detailed lane configuration plans for four strategies are illustrated in Figures 8–11. For strategy 1 (Figure 8), the one way street management strategy are used in all the internal segments, the additional turning restriction management strategy is used in intersection 6, 9, 24, and 27, besides the essential turning restriction for one way street management strategy. For strategy 2 (Figure 9), all turning arcs are permitted in each leg at each intersection and the number of lanes for each direction are equal in each segment. For strategy 3 (Figure 10), the left-turn restriction management strategy are used in each intersection. For strategy 4 (Figure 11), the one way street management strategy are used in all the internal segments.

Table VI summarizes the performance comparison results. Measures of effectiveness used for comparison include the multiplier value, the average travel distance of vehicles, and the maximum, average, and standard deviation of degrees of saturation for intersections and links.

One can observe from Table VI that the proposed model outperforms other three strategies in terms of enhancing the network capacity (i.e. significantly larger multiplier) because of its advantage of properly selecting and utilizing different types of traffic management strategies. Under the conventional design (Strategy 2), the average degree of saturation for intersections is almost the same as in Strategy 1, while the average degree of saturation for links is much lower, indicating that intersections comprise the major bottlenecks under Strategy 2 while the capacity of links is not fully utilized. The proposed model can reduce the number of bottleneck intersections and increase the capacity of intersections by reducing the number of signal phases and using links with low degrees of saturation as detour paths. Strategy 3 can reduce the average degree of saturation for intersections but shift worse congestion to less number of critical intersections that carry the detoured left-turn traffic

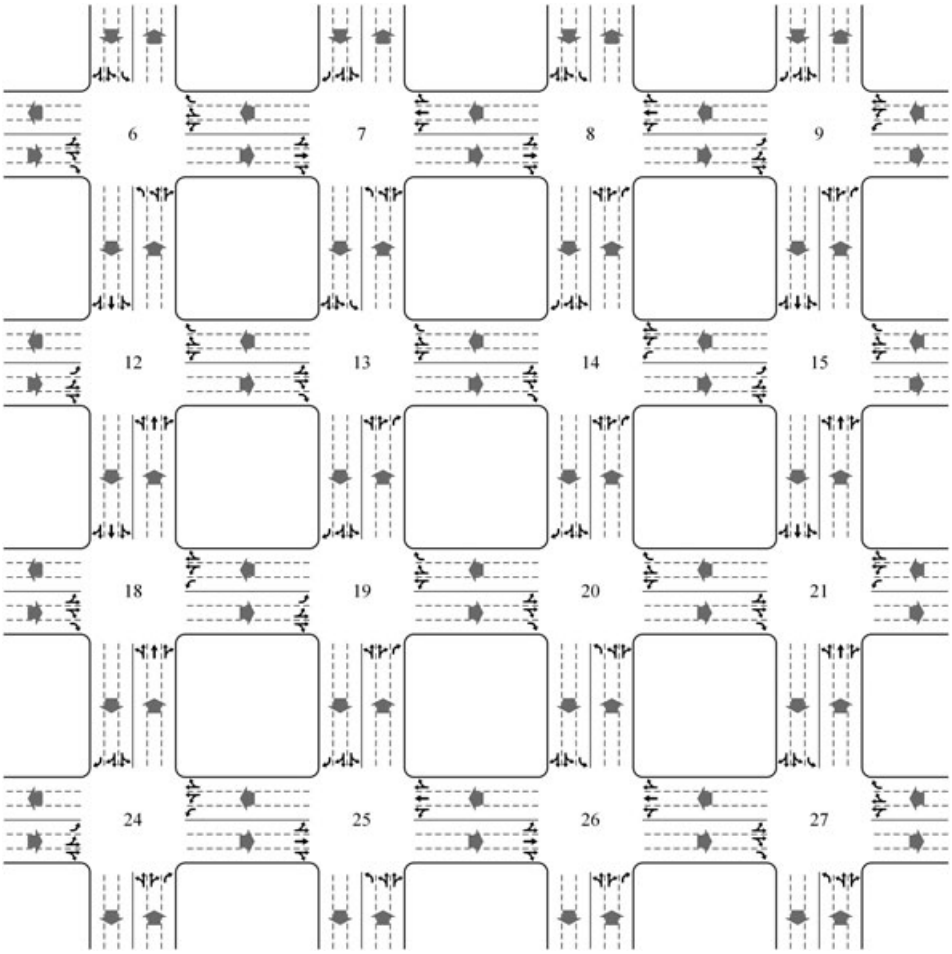

Figure 9. Optimized plans (Strategy 2).

DOI: 10.1002/atr

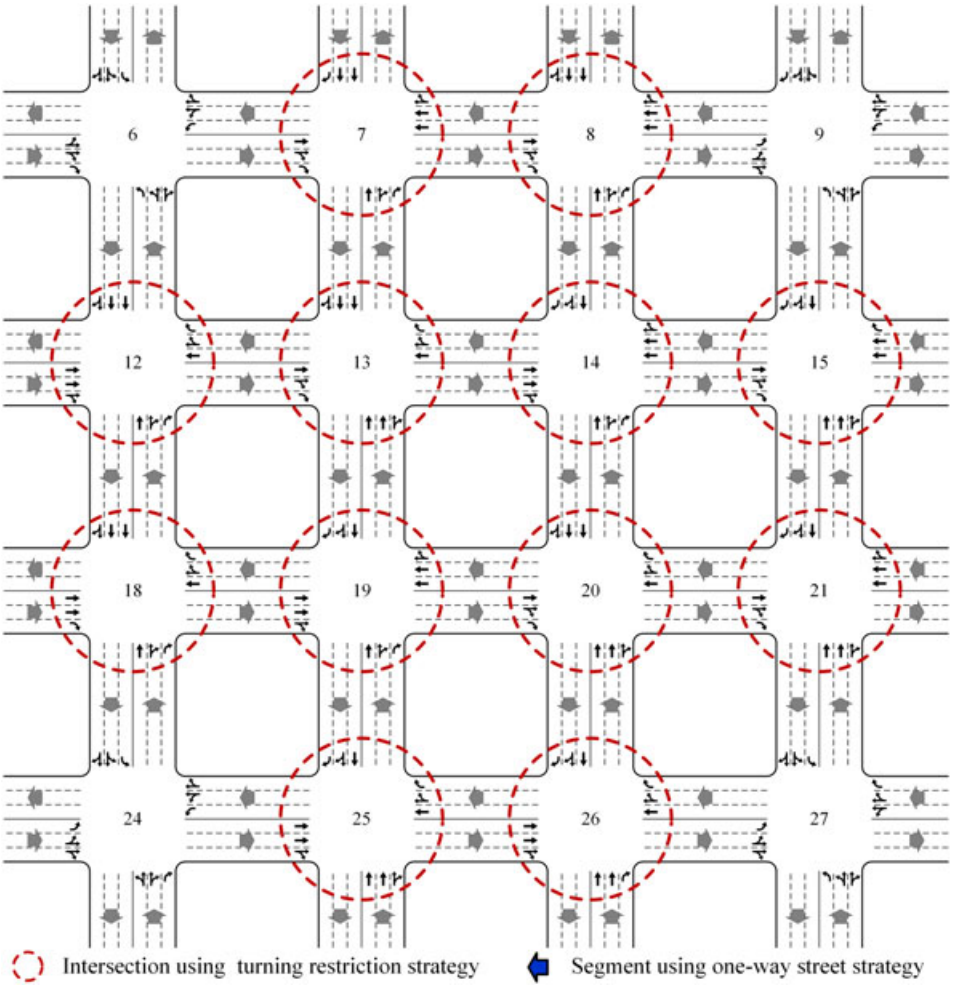

Figure 10. Optimized plans (Strategy 3).

(i.e. 6, 9, 24, and 27). Strategy 4 successfully reduces the degree of saturation at intersections and increases the network capacity; however the degree of saturation for links and the average travel distance of vehicles increase compared with the conventional design. Compared with Strategy 3 and Strategy 4, the proposed model yields significantly lower standard deviation of degrees of saturation for intersections, showing its capability of properly balancing the network load to prevent over-congestion at specific intersections.

Furthermore, the computational efficiency was analyzed. Table VII summarizes the comparison result of the CPU times under different network sizes.

6. FINDINGS

A lane-based optimization model integrating signal timings and reorganization of lane configurations is developed in this paper with the objective to enhance network capacity and relieve congestion. The model features a bi-level structure with a mix-integer-non-linear-programming problem at the upper-level and a parametric variational inequality at the lower-level. A GA-based heuristic is used to yield meta-optimal solutions [42] to the model.

Numerical analyses are conducted to evaluate the performance the proposed model. Comparisons are made between the proposed model and other candidate strategies such as conventional design, left-turn restriction system, and one-way street system. The following conclusions can be drawn:

DOI: 10.1002/atr

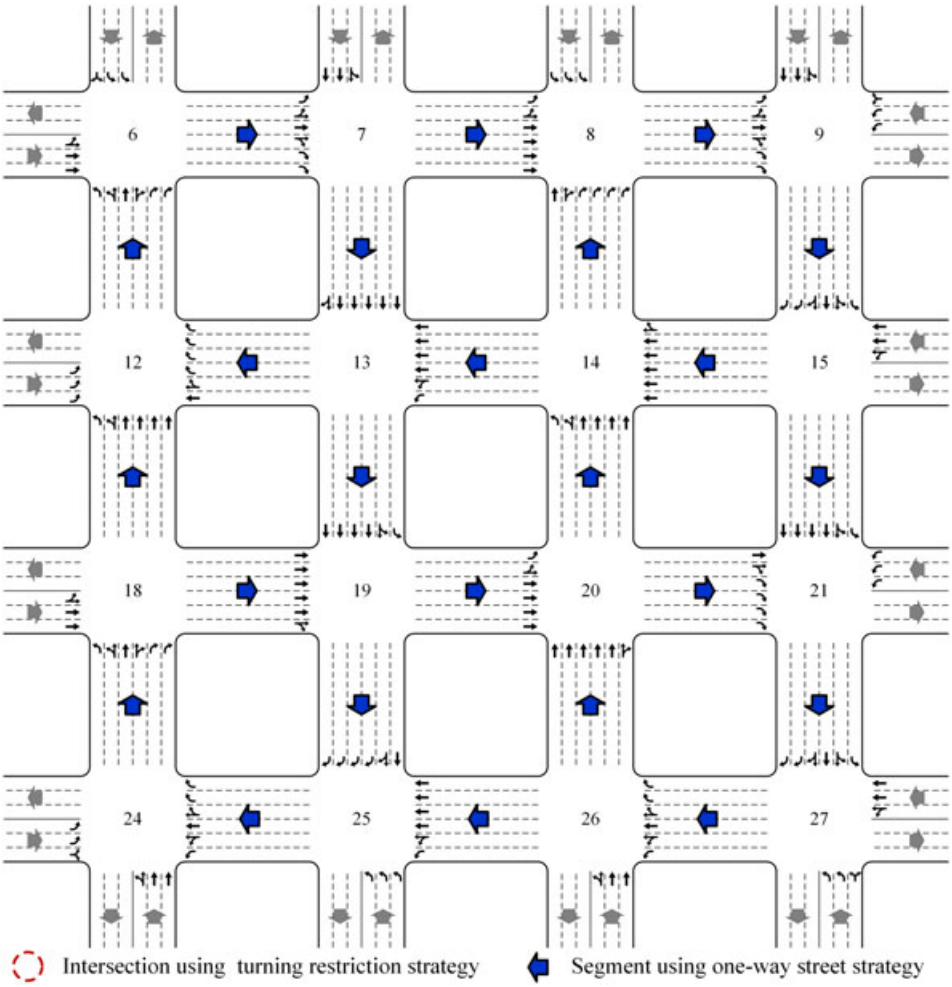

Figure 11. Optimized plans (Strategy 4).

Table VI. Performance comparison of different strategies.

Performance indices	Strategy 1	Strategy 2	Strategy 3	Strategy 4
Maximum μ	1.029	0.690	0.562	0.745
Maximum degree of saturation for intersections	0.900	0.900	0.900	0.900
Critical intersections	8, 12, 21, 25	6, 7, 8, 9, 12, 13, 14, 15, 18, 19, 20, 21, 24, 25, 26, 27	6, 9, 24, 27	6, 9, 24, 27
Average degree of saturation for intersections	0.879	0.899	0.606	0.724
Standard deviation of degree of saturation for intersections	0.027	0.000	0.175	0.105
Maximum degree of saturation for links	0.505	0.215	0.258	0.366
Average degree of saturation for links	0.320	0.194	0.195	0.239
Standard deviation of degree of saturation for links	0.093	0.009	0.039	0.069
Average travel distance (m)	3680	3040	3760	3640

DOI: 10.1002/atr

Table VII. Computational efficiency analysis.

Number of nodes	Computing time (min)
4	5
6	15
9	60
16	300
24	900
32	2200

1) The proposed model can optimize the lane reorganization and traffic control strategies in a unified framework. Compared with using them separately, integrated traffic management strategies may further expand the network capacity and improve the operational efficiency;
2) Compared with the conventional design, the proposed model can significantly reduce the number of bottleneck intersections and increase the capacity of the network by rerouting traffic and reducing the number of signal phases at intersections;
3) Compared with left-turn restriction and one-way street strategies, the advantage of the proposed model lies in its capability of properly balancing the network load to prevent over-congestion at specific intersections.

Because it is assumed that the segment between intersections, in this paper, is sufficiently long, the overflowing queue and weaving problems in the segment is neglected. Moreover, there is no real benefit for signal coordination because of platoon dispersion. In practice, if there involves two closely spaced intersections, the coordination of traffic signals must be considered [43]. Future work along the line will be extending the model into a dynamic setting and introduction of stochastic elements into the network flow patterns to accommodate the dynamic process of traffic control and management. Application and evaluation of the proposed model with a real-world transportation network will also be performed in the next step.

ACKNOWLEDGGEMENTS

The research is supported by the National Natural Science Foundation of China under Grant No.51238008 and the PhD research startup foundation of University of Shanghai for Science and Technology (No. BSQD201504).

REFERENCES

1. Wolshon PB, Lambert L. Convertible roadways and lanes: a synthesis of highway practice. NCHRP Synthesis 340, Transportation Research Board, Washington, DC, 2004.
2. Yu X, Prevedouros PD. Left-turn prohibition and partial grade separation for signalized intersections: planning-level assessment. *Journal of Transportation Engineering* 2013; **139**(4): 399–406.
3. Bonneson JA, Fontaine MD. Engineering study guide for evaluating intersection improvements. NCHRP Report 457, Transportation Research Board, Washington, DC, 2001.
4. Long J, Gao Z, Zhang H Szeto WY. A turning restriction design problem in urban road networks. *European Journal of Operational Research* 2010; **206**(3): 569–578.
5. Guang X, Wu L. A model of the urban road intersection left-turning restriction. *Journal of Theoretical and Applied Information Technology* 2013; **48**(3): 1619–1625.
6. Cova TJ, Johnson JP. A network flow model for lane-based evacuation routing. *Transportation Research Part A: Policy and Practice* 2003; **37**(7): 579–604.
7. Liu Y, Luo Z. A bi-level model for planning signalized and uninterrupted flow intersections in an evacuation network. *Computer-Aided Civil and Infrastructure Engineering* 2012; **27**(10): 731–747.
8. Xie C, Lin D Waller ST. A dynamic evacuation network optimization problem with lane reversal and crossing elimination strategies. *Transportation Research Part E: Logistics and Transportation Review* 2010; **46**(3): 295–316.
9. Xie C, Turnquist MA. Lane-based evacuation network optimization: an integrated Lagrangian relaxation and tabu search approach. *Transportation Research Part C: Emerging Technologies* 2011; **19**(1): 40–63.
10. Nava E, Shelton J, Chiu YC. Analyzing impacts of dynamic reversible lane systems using a multi-resolution modeling approach, 91st Annual Meeting of the Transportation Research Board, Washington, DC, 2012.
11. Wojtowicz J, Wallace WA. Traffic management for planned special events using traffic microsimulation modeling and tabletop exercises. *Journal of Transportation Safety & Security* 2010; **2**(2): 102–121.

DOI: 10.1002/atr

12. Williams BM, Tagliaferri AP, Meinhold SS, Hummer JE Rouphail NM. Simulation and analysis of freeway lane reversal for coastal hurricane evacuation. *Journal of Urban Planning and Development* 2007; **133**(1): 61–72.
13. Ren G, Hua J, Cheng Y, Zhang Y Ran B. Bus contraflow lane: improved contraflow approach in freeway evacuation. *Transportation Research Record* 2012; **2312**: 150–158.
14. Yang H, Bell M. Models and algorithms for road network design: a review and some new developments. *Transport Reviews* 1998; **18**(3): 257–278.
15. Zhang H, Gao Z. Two-way road network design problem with variable lanes. *Journal of Systems Science and Systems Engineering* 2007; **16**(1): 50–61.
16. Kalafatas G, Peeta S. Planning for evacuation: insights from an efficient network design model. *Journal of Infrastructure Systems* 2009; **15**(1): 21–30.
17. Karoonsoontawong A, Lin D. Time-varying lane-based capacity reversibility for traffic management. *Computer-Aided Civil and Infrastructure Engineering* 2011; **26**(8): 632–646.
18. Dorroh RF, Kochevar RA. One-way conversions for calming Denver's Streets, 1996 ITE International Conference, Dana Point, California, 1996, 109–113.
19. Vo PT, Mattingly SP, Ardekani S Dilshad Y. Comparison of quality of service in two central business districts: two-fluid model approach in Texas. *Transportation Research Record* 1999; **2007**: 180–188.
20. Chiu Y, Zhou X Hernandez J. Evaluating urban downtown one-way to two-way street conversion using multiple resolution simulation and assignment approach. *Journal of Urban Planning and Development* 2007; **133**(4): 222–232.
21. Gayah VV, Daganzo CF. Analytical capacity comparison of one-way and two-way signalized street networks. *Transportation Research Record* 2012; **2301**: 76–85.
22. Tuydes H. *Network Traffic Management Under Disaster Conditions*. Northwestern University: Chicago, 2005.
23. Shi F, Huang E, Chen Q Wang Y. Optimization of one-way traffic organization for urban microcirculation transportation network. *Journal of Transportation Systems Engineering and Information Technology* 2009; **9**(4): 30–35.
24. Long D, Shi F Wang Y. One-way traffic organization based on traffic load and road equity. *Journal of Transportation Systems Engineering and Information Technology* 2010; **10**(6): 109–114.
25. Lam WH, Poon AC Mung GK. Integrated model for lane-use and signal-phase designs. *Journal of Transportation Engineering* 1997; **123**(2): 114–122.
26. Wong CK, Wong SC. Lane-based optimization of signal timings for isolated junctions. *Transportation Research Part B: Methodological* 2003; **37**(1): 63–84.
27. Wong CK, Heydecker BG. Optimal allocation of turns to lanes at an isolated signal-controlled junction. *Transportation Research Part B: Methodological* 2011; **45**(4): 667–681.
28. Wong SC, Yang H. Reserve capacity of a signal-controlled road network. *Transportation Research Part B: Methodological* 1997; **31**(5): 397–402.
29. Wong CK, Wong SC. Lane-based optimization of traffic equilibrium settings for area traffic control. *Journal of Advanced Transportation* 2002; **36**(3): 349–386.
30. Cantarella GE, Pavone G Vitetta A. Heuristics for urban road network design: lane layout and signal settings. *European Journal of Operational Research* 2006; **175**(3): 1682–1695.
31. Chen A, Yang H, Lo HK Tang W. A capacity related reliability for transportation networks. *Journal of Advanced Transportation* 1999; **33**(2): 183–200.
32. Chootinan P, Wong SC Chen A. A reliability-based network design problem. *Journal of Advanced Transportation* 2005; **39**(3): 247–270.
33. Chen A, Chootinan P Wong SC. New reserve capacity model of a signal-controlled road network. *Transportation Research Record* 1964; **2006**: 35–41.
34. Chen A, Kasikitwiwat P Yang C. Alternate capacity reliability measures for transportation networks. *Journal of Advanced Transportation* 2013; **47**(1): 79–104.
35. Chiou SW. Reserve capacity of signal-controlled road network. *Applied Mathematics & Computation* 2007; **190**(2): 1602–1611.
36. Wong CK, Wong SC Lo HK. Reserve capacity of a signal-controlled network considering the effect of physical queuing. In *Proceedings of the 17th International Symposium of Transportation and Traffic Theory*, (Eds)Elsevier: London, 2007.
37. Heydecker BG. *Sequencing of Traffic Signals, Mathematics in Transport and Planning and Control*. Clarendon Press: Oxford, 1992 57–67.
38. Wang S, Meng Q Yang H. Global optimization methods for the discrete network design problem. *Transportation Research Part B: Methodological* 2013; **50**: 62–60.
39. Fisk C, Nguyen S. Solution algorithms for network equilibrium models with asymmetric user costs. *Transportation Science* 1982; **16**(3): 361–381.
40. Gen M, Cheng R. *Genetic Algorithms and Engineering Optimization*. John Wiley & Sons: New York, 2000.
41. Cormen TH, Leiserson CE, Rivest RL Stein C. *Introduction to Algorithms*. MIT Press: Cambridge, Massachusetts, 2001.
42. Golberg DE. *Genetic Algorithms in Search, Optimization, and Machine Learning*. Addion Wesley: Boston, Massachusetts, 1989.
43. Wong CK, Wong SC Lo HK. A spatial queuing approach to optimize coordinated signal settings to obviate gridlock in adjacent work zones. *Journal of Advanced Transportation* 2010; **44**(4): 231–244.

DOI: 10.1002/atr